Microfluidic study of effects of flow velocity and nutrient concentration on biofilm accumulation and adhesive strength in microchannels

Na Liu,[a]# Tormod Skauge,[a]* David Landa-Marbán,[b] Beate Hovland,[a] Bente Thorbjørnsen,[a] Florin Adrain Radu,[b] Bartek Florczyk Vik,[a] Thomas Baumann,[c] Gunhild Bødtker[a]

[a]Uni Research, Realfagbygget, Centre for Integrated Petroleum Research (CIPR), Nygårdsgaten 112, 5008 Norway

[b]Department of Mathematics, Faculty of Mathematics and Natural Sciences, University of Bergen, Allégaten 41, P.O. Box 7803, 5020 Bergen, Norway.

[c]Institute of Hydrochemistry, Technische Universität München, Marchioninistr. 17, D-81377 München, Germany

Running Head: Biofilm accumulation and adhesive strength

#Address correspondence to Na Liu, nali@norceresearch.no.

*Present address: Tormod Skauge, Energy Research Norway, Realfagbygget, Allégaten 41, Bergen 5007, Norway.

ABSTRACT

Biofilm accumulation in the porous media can cause plugging and change many physical properties of porous media. Up to now, applications of desired biofilm growth and its

subsequent bioplugging have been attempted for various practices. A deeper understanding of the relative influences of hydrodynamic conditions including flow velocity and nutrient concentration, on biofilm growth and detachment is necessary to plan and analyze bioplugging experiments and field trials. The experimental results by means of microscopic imaging over a T-shape microchannel show that flow velocity and nutrient concentrations can have significant impacts on biofilm accumulation and adhesive strength in both flowing and stagnant microchannels. Increase in fluid velocity could facilitate biofilm growth, but that above a velocity threshold, biofilm detachment and inhibition of biofilm formation due to high shear stress were observed. High nutrient concentration prompts the biofilm growth, but was accompanied by a relatively weak adhesive strength. This research provides an overview of biofilm development in a hydrodynamic environment for better predicting and modelling the bioplugging associated with porous system in petroleum industry, hydrogeology, and water purification.

IMPORTANCE

In the recent decade, the use of bacteria has become more and more important in many applications. Bioplugging caused by bacteria growth in porous media has been explored as a viable technique for some applications, such as bioremediation, water purification and microbial enhanced oil recovery (MEOR). In order to control biofilms/biomasses selectively/directionally plugging in desirable places, the role of hydrodynamic conditions on biofilm growth and detachment is essential to investigate. Herein, a T-shape microchannel was prepared to study effects of flow velocity and nutrient concentration on biofilm accumulation and adhesive strength at pore scale. Our results

47 suggest that flow velocity and nutrient concentration could control biofilm accumulation
48 in microchannels. The finding helps explain and predict the engineering bioplugging in
49 porous media, especially for the selective plugging strategy of a MEOR field trial.

50 **INTRODUCTION**

51 Biofilm accumulation in the pore space can cause pore plugging, leading to significant
52 changes in physical properties of porous media, such as the reduction of porosity and
53 permeability (1-5). The plugging effect might have negative impacts in many industrial
54 and medical applications because the clogging pores need extra cost to clean and
55 prevention. However, engineering bioplugging has been explored as a viable technique
56 for various practices, such as in situ bioremediation (6), soil injection (7), waste treatment
57 (8, 9), ground water recharge (10) and microbial enhanced oil recovery (11-15). For
58 example, in MEOR trails biofilm accumulation leads to selective plugging of high
59 permeability zones, subsequently forcing the diversion of injected fluids towards lower
60 permeable zones to improve the oil recovery (15, 16). Suthar et al. confirmed the
61 obtained oil recovery because of bacterial growth and biofilm formation in the sand pack
62 (17). Karambeigi et al. used two different heterogeneous micromodels to observe
63 potential of bioplugging of high permeable layers of porous media for improving the
64 efficiency of water flooding (2). Klueglein et al. investigated the influences of nutrients
65 concentrations on cell growth and bioplugging potential during a MEOR trial (18). Even
66 tremendous efforts have been made to improve the understanding of bioplugging, few
67 works concern biofilm studies of biofilm growth and detachment mechanisms
68 accompanying the bioplugging process.

Bioplugging in porous media results from the accumulation of bacterial cells, production of extracellular polymeric substances (EPSs) in the pore space. Due to physicochemical properties of EPSs, biofilms can behave as viscous liquids to resist the flow-induced shear stress, and substantially plug the pore (19-22). Engineering bioplugging is a process used to control biofilms selectively and substantially plugging in desired places (6, 23, 24). Therefore, knowledge on mechanisms of biofilm development and its adhesive strength with solids surface is vitally important to plan and predict the engineering bioplugging process. It was found that biofilm growth and detachment could be significantly influenced by varying hydrodynamic conditions on the surrounding environment (19, 20, 25). Biofilm growth and detachment rates could both increase with fluid velocity, as the increased mass transfer facilitating nutrients supply for bacteria growth, while the increased shear force in turn causing detachment (19, 21, 26, 27). There is a consensus that biofilm growth rate increases with nutrients concentration, while nutrient starvation results in biofilm detachment (28-30). Nonetheless, knowledge on bioplugging must be depicted by examining a correlation between biofilm accumulations and its adhesive strength and hydrodynamic conditions like flow velocity and nutrient concentration, to improve understanding and hence ability to control bioplugging in fluid flooded porous systems.

Traditionally quiescent experiments for biofilm research were normally carried on homogeneous physical conditions, which lack environmental complexities for accurately determining the dynamic changes occurring during biofilm development (31). The advent of new technologies, specially microfluidics, have attracted a rapidly growing interest to emulate biological phenomena by addressing unprecedented control over the flow

conditions, providing identical and reproducible culture conditions, as well as real-time observation (26, 30, 32, 33). Indeed, microfluidics has been used for observing biofilm formation under various fundamental and applied researches, e.g. wastewater treatment (34) and medical fields (20, 35). Herein, we used a T-shape microfluidic device equipped with a microscope to study the biofilm accumulation and adhesive strength as responds to various flow velocities and nutrient concentrations in the microchannel.

RESULTS

Effects of flow velocity on biofilm accumulation and adhesive strength. Biofilms development in microchannels were measured by varying injecting flowrates of 10mM pyruvate (1.0 N) from 0.2 µl/min to 0.5 µl/min. After 6 days, the shear rate was steadily increased to 500.00 s^{-1} to test the adhesive strength of biofilm attached on the solid surface. The corresponding flow velocity, Peclet number, Reynolds number and shear rate at each flowrate in Channel 1 are listed in **Table 1**.The accumulation of biofilms at different velocities was observed and registered as function of time by use of microscope.

TABLE 1. Table of basic flow parameters at various flowrates in this study.

Flowrate, µl/min	Water velocity, mm/s	Peclet number, Pe	Reynolds number, Re	Shear rate, s^{-1}
0.2	1.66	97.64	0.17	83.33
0.3	2.50	147.06	0.25	125.00
0.4	3.33	195.88	0.33	166.67
0.5	4.17	245.30	0.42	208.33

1.2	10.00	705.88	1.00	500.00

107

108 B**iofilm morphologies.** Images of biofilms development in two microchannels at various
109 flow velocities are shown in **Fig. 2**. After inoculation, the initial attached biofilms at low
110 velocities (1.66 and 2.50 mm/s) became irreversible and developed towards different
111 structures along the nutrients flow. Biofilms at 1.66 mm/s tends to be approximately
112 circular shape and has a larger coverage area, while biofilms at 2.50 mm/s show
113 appearance of thin plate structures. There is no clear biofilm formation in Channel 1 at
114 high velocities. On the contrary, biofilms formed at Channel 2 at 3.33 mm/s led to a
115 larger clusters compared with low rates. There was no biofilm growth in either channel at
116 the highest flow velocity of 4.17 mm/s.
117 After 6 days of biofilm culturing, the shear rate steadily increased to 500.00 s^{-1} to test the
118 adhesive strength between biofilms and solid surfaces. As shown in the right column
119 images of **Fig. 2**, biofilms in Channel 1 at 1.66 mm/s became elongated in the flowing
120 direction to form filamentous “streamers” when the shear force acting on biofilms
121 increasing with shear rate; while there was no clear shape difference on biofilms growth
122 at higher velocities in Channel 1 and Channel 2.

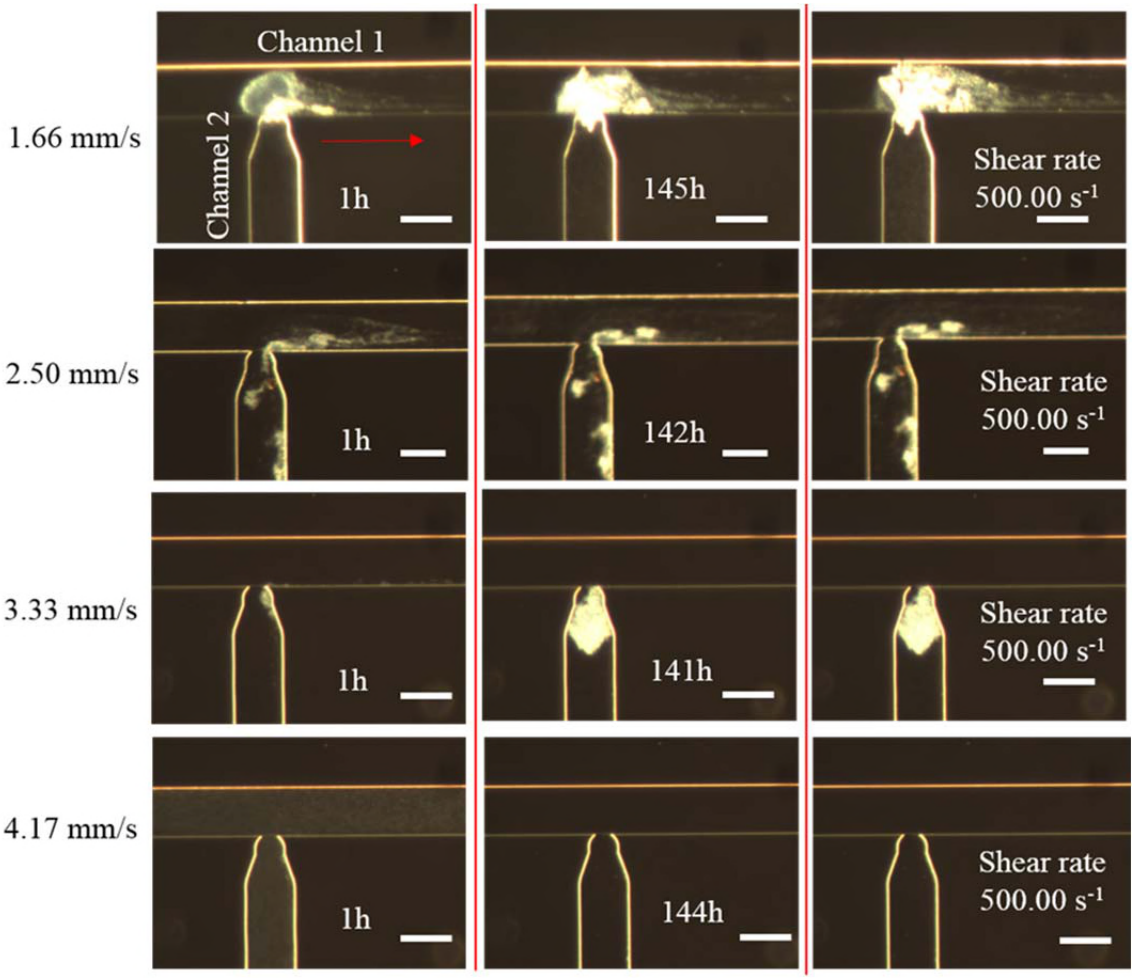

FIG 2. Optical images of biofilm growth in both microchannels at 1.0 N and various velocities. Images in the left column were taken after injecting nutrients for 1 h. The middle column shows images of biofilm growth for around 6 days. The right column lists images of biofilm detachment by increasing shear rate to 500.00 s^{-1}. Nutrients flow from right to left in the upper channel. Scale bars indicate 100 μm.

Biofilm accumulation in the flowing and no-flowing channels. Biofilm coverages as a function of time for different flow velocities in two microchannels are listed in **Fig. 3**. In the early of injection, the coverage of biofilms decreased as the flow shear stress snapped off some of weak initial attachments. After an active time when the left biofilms turned into irreversibly attached and new biofilms formed, biofilms coverage increased over

time. As the velocity increased from 1.66 to 4.17 mm/s, biofilm coverage gradually decreased. **Fig. 3 (b)** plots biofilm coverage in the no flowing channel (Channel 2) as a function of time in each run. Biofilm coverages at all velocities increased over time, while the optimum velocity is 3.33 mm/s due to its exceptionally high accumulation rate.

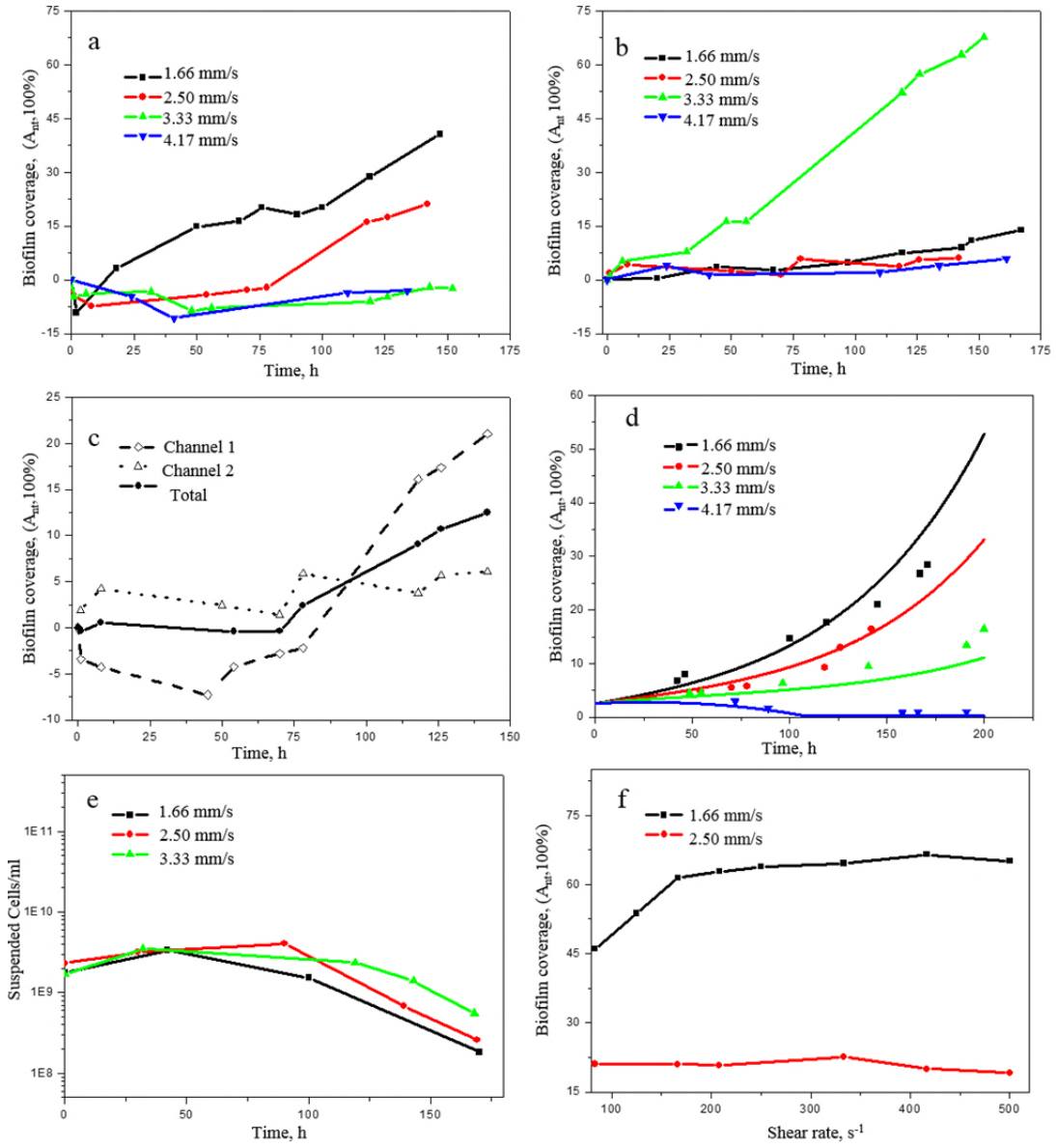

FIG 3. (a) Biofilm coverage over time in Channel 1 at various velocities; (b) Biofilm coverage over time in Channel 2 at different velocities; (c) Comparison of biofilm

accumulation in both channels at 2.50 mm/s; (d) Experimental data and numerical simulations of biofilm coverage in both channels at various velocities; (e) Number of released cells as a function of biofilm culture time at various velocities; (f) Biofilm coverage in Channel 1 as response to the increasing shear rate after culturing biofilms at the velocities of 1.66 and 2.50 mm/s for 6 days.

Comparing biofilms growth at 2.50 mm/s in Channel 1 and Channel 2 in **Fig. 3 (c)**, biofilm coverage in Channel 2 increased with time initially but after 75 hours reached to a plateau value. This leveling off behavior was not observed in Channel 1. The stable coverage obtained in Channel 2 might be attributed to that cells in the biofilm cannot obtain sufficient essential sources of nutrients for new biofilm formation as biomass increased in the growing biofilm community. However, the continuous nutrients supply in Channel 1 delays this plateau. **Fig. 3 (d)** compares the experimental data with the mathematical model of biofilm coverages in both microchannels at various velocities. The numerical data is from D. L. Marbán' work (D. L. Marbán, submitted for publication) , and shows that our experiment data is well fit with the numerical simulation.

B**iofilm adhensive strenth test.** In the biofilm culturing time, the number of released bacterial cells in the effluent at various velocities is shown in **Fig. 3 (e)**. The cells number increased in the first two days after inoculation, which mainly contributes to that the reversible adhered bacteria after inoculation were driven out the microchannel by the nutrients flow shear stress. After 48 h, the biofilm-dispersal cells decreased, which corresponds to the increase of biofilm coverage over time in **Fig. 3 (a)**, exhibiting that more bacteria involved into biofilm growth. Moreover, the increase of cell densities with

flow velocity may indicate a higher detachment rate and a possible higher planktonic growth with an increase of shear stress.

After 6 days of biofilm culturing, biofilm coverages in Channel 1 as responds to the increasing shear rate from 83.33 s^{-1} and 125.00 s^{-1} up to 500.00 s^{-1} are shown in **Fig. 3 (f)**. Biofilm accumulation at 1.66 mm/s increased when increasing nutrients shear rate to 166.67 s^{-1}, suggesting that the increasing shear stress facilitates the diffusion of nutrients inside of biofilm and promotes its growth. Continuely increasing the shear rate, the growth trend slowed down; until up to 500 s^{-1}, biofilm coverage slightly decreased, which dominates that the high shear rate brought about biofilm detachment. Simillar results are obtained at biofilm growth at 2.50 mm/s, which no large degree of detachment occurred as responds to low flow shear rates until up to 500 s^{-1}.

Effect of nutrient concentration on biofilm accumulation and adhesive strength. To assess the influence of nutrient conditions on biofilm accumulation and adhesive strength, biofilms were cultured at different nutrient concentrations. The baseline, 1.0 N, was 10 mM pyruvate in the growth medium and variations of two times (2.0 N), half (0.5 N) and one tenth (0.1 N) of the baseline concentration were applied. Injections were performed at a constant velocity of 1.66 mm/s from Channel 1 for approximately 7 days, and followed by a biofilm strength test by steadily increasing shear rate. The images are shown in **Fig. 4**.

B**iofilm morphologies.** As shown in **Fig. 4**, biofilm in Channel 1 with the highest concentration 2.0 N has a long, thick but loose structure, which is highly sensitive to the variation of shear stress. After 122 h, the formed biofilm was dispersed from the deep of the matrix, leaving behind a few attached biofilm spots to regrow. At nutrients input 1.0

187 N and 0.5 N, biofilm became denser and compacted, and the influence of shear stress
188 reduced. When decreasing the nutrient concentration to 0.1 N, there was no clear biofilm
189 growth occurred in the nutrient continuous flowing channel.

190 The biofilm in Channel 2 at nutrient inputs of 2.0 N and 0.5 N had larger coverages than
191 other concentrations, which the former confirms that high nutrient concentrations lead to
192 a fast biofilm growth and the later might be related to the large initial attachments
193 containing more biomasses for biofilm growth. It is noticed that there is barely new
194 biofilm formation at both channels at 0.1 N, which shows that the lowest nutrient input
195 significantly limited biofilm growth and formation.
196 As responding to the increasing shear rate, biofilm with low density and loose structure at
197 2.0 N, wars highly sensitive to the variation of shear stress, which detached from the
198 substrates at the shear rate of 83.33 s^{-1}. Biofilm growth at 0.5 N reacted as same as that at
199 1.0 N when the increasing shear rate acted on biofilms, and became elongated in the
200 flowing direction.

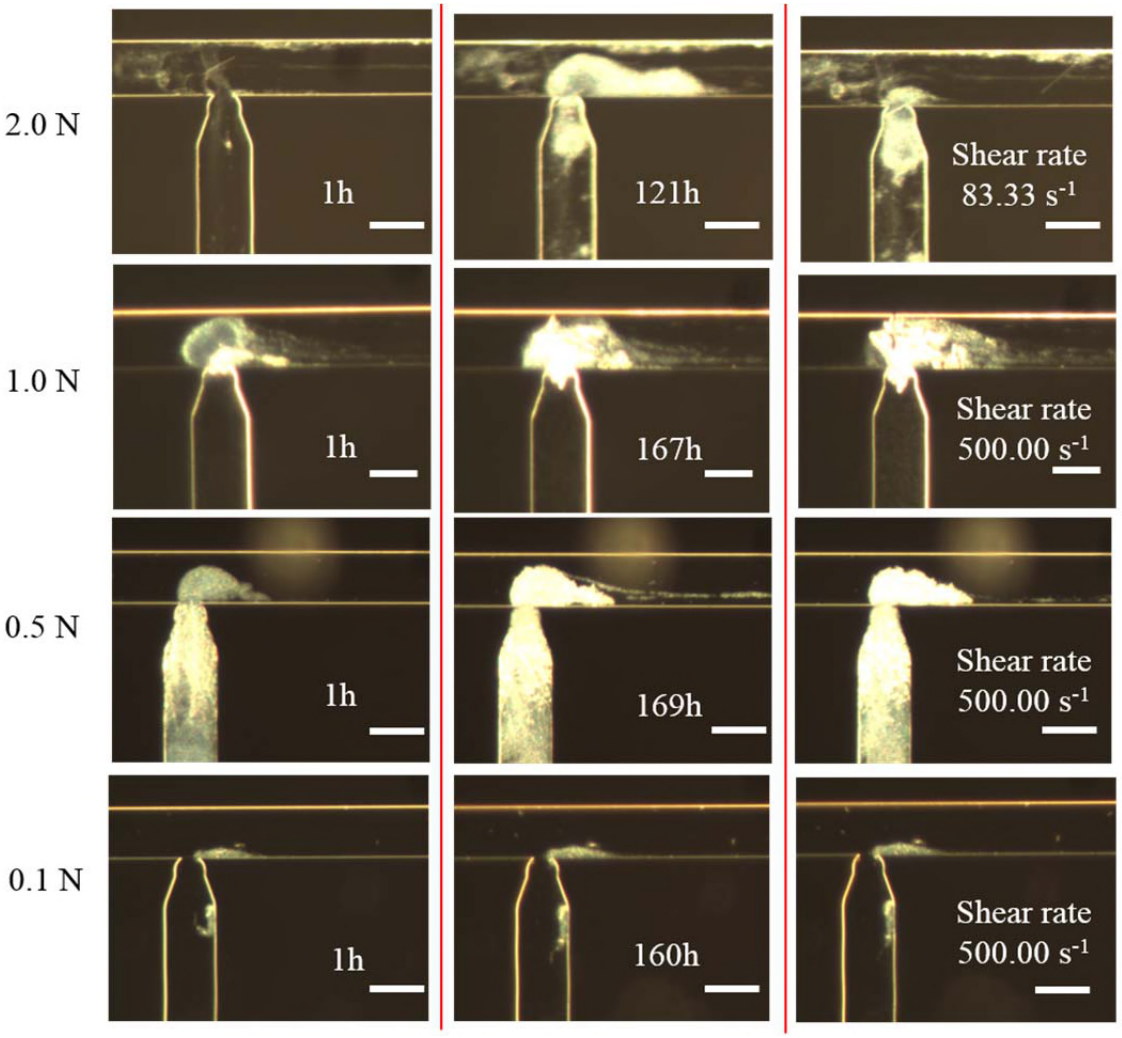

FIG 4. Optical images of biofilm growth over time at various nutrient concentrations, 2.0 N, 1.0 N, 0.5 N, and 0.1 N, respectively. Images in the left column were taken after injecting nutrients for 1 h. The middle column shows images of biofilm growth for around 7 days. The right column lists images of biofilm detachment by increasing shear rate to 500.00 s^{-1}. Nutrients flow from right to left in the upper channel. Scale bars indicate 100 μm.

Biofilm accumulation in the flowing and no-flowing channels. Biofilm coverages as a function of time for different nutrient concentrations in two microchannels are shown **Fig. 5**. As shown in **Fig. 5 (a)**, in Channel 1, biofilm growth at a high nutrient

211 concentration of 2.0 N has a much faster accumulation rate in the first 5 days, but rapidly
212 decreased when most parts of biofilm matrix were detached from the substrate. At the
213 medium nutrient feeding zones, biofilm accumulation at 0.5 N is higher than that of 1.0 N
214 in the first 3 days, and reached a plateau value after that, which was not observed for 1.0
215 N. When decreasing the nutrient concentration to 0.1 N, there was no clear biofilm
216 formation in both channels. Therefore, the lowest nutrient concentration (0.1 N) could not
217 provide environment for biofilm growth. In this study, the limiting nutrient concentration
218 for biofilm growth appears to be between 0.1 and 0.5 times N.

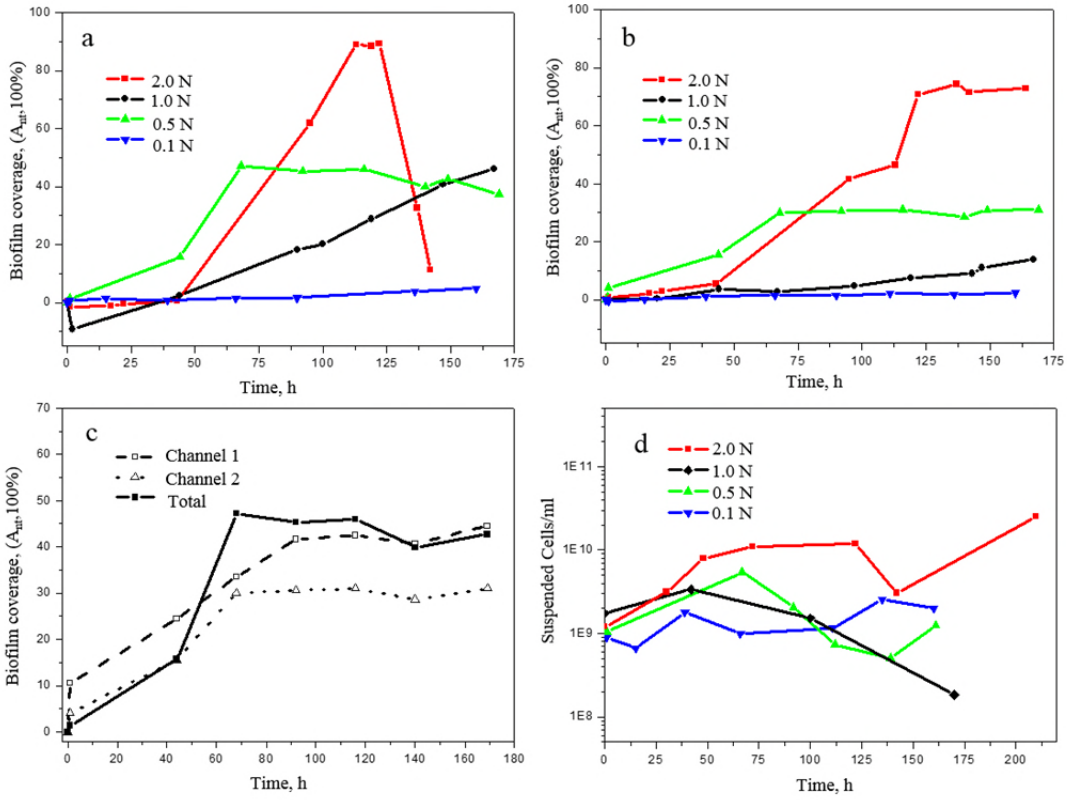

219

220 **FIG 5.** (a) Biofilm coverage over time in Channel 1 at different nutrient concentrations;
221 (b) Biofilm coverage over time in Channel 2 at different nutrient concentrations; (c)
222 Comparison of biofilm coverage in both channels at 0.5 N and 1.66 mm/s; (d) Cell
223 number of effluents at various nutrient concentrations at the flow velocity of 1.66 mm/s.

As shown in **Fig. 5 (b)**, biofilm accumulation in Channel 2 is influenced by nutrient concentrations. Biofilm formation at 2.0 N has larger coverage than other cases, indicating that high nutrients loading in Channel 1 leads to an increase in biofilm growth in Channel 2. In addition, biofilm growth in a no flow channel reached to a stable plateau at the later stage of its development. The time to reach the stable plateau at 2.0 N was later than 0.5 N, suggesting that high nutrient concentration leads to a decrease in the time taken to reach the stable plateau in a no flow system. **Fig. 5 (c)** shows that biofilm coverage obtained stable plateaus at 0.5 N in both channels. The time to reach the plateau in Channel 1 was later than that in Channel 2, indicating that flow shear rate can facilitate mass transfer and lead an increase in the time taken to reach the stable state.

B**iofilm adhesive strength test. Fig. 5 (d)** presents the result of cell number in the effluent at different nutrient concentrations. The cell number at 2.0 N is higher than other nutrient concentrations. The released cell numbers are relatively in the same level at 0.5 N and 1.0 N in the beginning. However, when biofilm stopped growing at 0.5 N, the detached cells increased over time, suggesting that the mature biofilm would disperse more planktonic cells into the bulk liquid (26). At the limited nutrient supply (0.1 N), the released cell number in the effluent was stable and no biofilm accumulated in the channel, indicating that bacteria at limited nutrient loading prefer to live in the planktonic style instead of biofilm style (36, 37).

It is noticed that biofilm growth at 2.0 N had a weak adhesive strength with substrates, because cells deep in the biofilm were dispersed from the interior of the biofilm matrix causing large degree of detachment. We observed this dispersion occurring at nutrient concentration of 2.0 N and flow velocities of 1.66 and 2.50 mm/s (**Fig. 6 (a)**). Firstly, a

central region in the biofilm matrix (shows in red circles of images in **Fig. 6 (a)**), become visible and light, which has demonstrated the pre-dispersion behavior (22). Eventually, microcolonies within the regions migrated into the bulk liquid, leading to huge biofilm detachments. Biofilms were observed to undergo growth and dispersion simultaneously at high nutrient concentrations (**Fig. 6 (b)**). The coverage area increased steadily after an active time, but decreased when biofilms were detached from the substrate and increased again while the left biofilm spots regrew. As biofilm growth at high rate at 2.0 N, cells trapped deeper in the biofilm matrix may have difficulties obtaining essential sources of energy or nutrients. In addition, waste products and toxins can accumulate fast in the biofilm community to reach toxic levels, threatening cells survival. Thus, microorganisms within the biofilm release from the matrix to resettle at a new location.

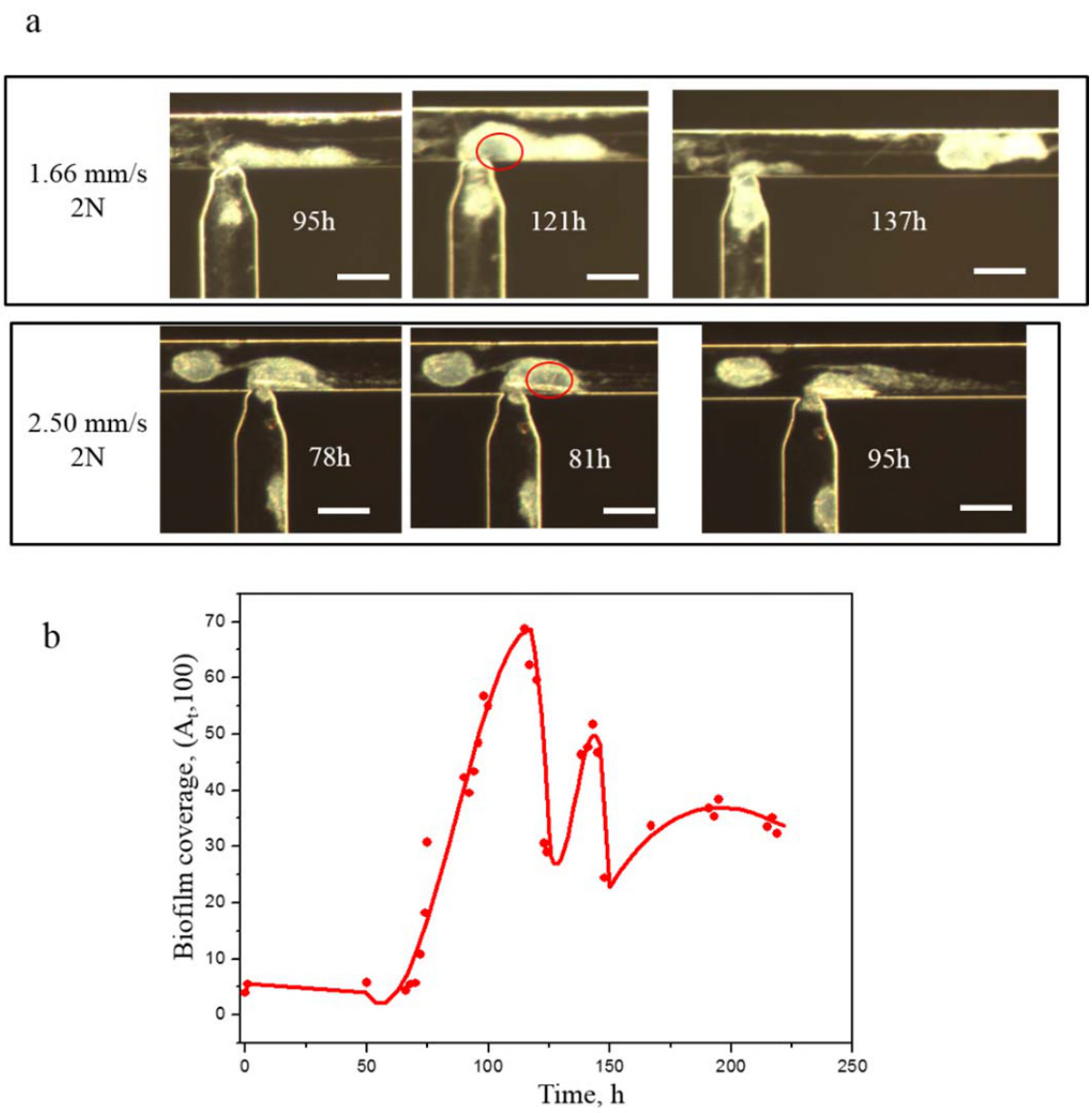

FIG 6. (a) Images of biofilm growth following dispersion events at high nutrient concentration of 2.0 N and flow velocities at 1.66 and 2.50 mm/s. (b) Biofilm accumulation at 1.66 mm/s and nutrient concentration of 2.0 N.

DISCUSSION

Biofilm morphologies. The observations on biofilm morphologies at each run demonstrate that flow velocity and nutrients concentration have direct effects on biofilm morphology. Biofilms formed in Channel 1 reveal the influence of flow shear stress drag.

266 The shapes of biofilm clusters became compacted and progressively elongated along the
267 flow direction with the increase of flow velocity (**Fig. 2**). While biofilms formed at the
268 high nutrient concentration have long, thick but loose structures, and became denser and
269 compacted with the decrease of nutrient loading (**Fig. 4**). Similar results have been
270 reported in previous work (21).
271 Biofilm growth in Channel 2 is highly dependent on the diffusion of nutrients in Channel
272 1. As the former bacteria injection path, most parts of Channel 2 were full of biomasses
273 without fluid shear forces. Only the void in the nozzle connecting with Channel 1 could
274 act as the transport channel supplying nutrients for biofilm growth. Biofilms at the high
275 shear rate of 166.67 s^{-1} and 2.0 N led to larger clusters compared with others, indicating
276 that shear rate and nutrient concentration in Channel 1 determined the flux of nutrients
277 transport to Channel 2.
278 It is noticed that there was no biofilm growth in either channel at the highest flow
279 velocity of 4.17 mm/s and lowest nutrients concentrations of 0.1 N, suggesting that the
280 high shear forces and limited nutrients loading may prevent biofilm formation, which is
281 in agreement with industrial applications where the formation of biofilm is prevented by
282 high velocity flooding (36).
283 **Biofilm accumulation in the microchannel.** In this study, we set the initial biofilm
284 coverage after inoculation to zero, and plot biofilm net coverage A_{nt}, by subtracting initial
285 attachment to analysis biofilm accumulation. As shown in **Fig. 3 (a)** and **Fig. 5 (a)**, the
286 coverages of biofilm are under zero in Channel 1 in the early stage of injection, which
287 demonstrates that the shear stress caused by nutrients flowing leads to snap-off of weak
288 initial attachments. When the remained biofilms became irreversibly attached, they

289 behaved as nuclei for new bacteria/biofilm growth, resulting in the increase of biofilm
290 coverage. Biofilm accumulation in the flowing microchannel (Channel 1) is highly
291 related with flow velocities through two important factors, mass transfer and shear stress
292 (19, 27). As shown in **Table 1**, the Reynolds numbers in Channel 1 were very low (from
293 0.17 to 0.42), while the mass transfer Peclet number were extremely high (from 97.64 to
294 245.30), which suggests that mass transfer in the microchannel was dominated by
295 convective actions and has negligible diffusion (38). Thereby, the diffusion of nutrients
296 from bulk to biofilms rarely increased when increasing the flow velocity, while the shear
297 stress caused by water flow increased linearly. The accumulation of biofilm, which is
298 equal to its growth rate minus detachment rate, decreased with increasing flow velocities
299 when the shear stress induced detachment rate exceed growth rate. Thereby, the optimum
300 flow velocity for biofilms growth in the flow microchannel is the lowest velocity of 1.66
301 mm/s in this work.
302 The effect of nutrient concentration on biofilm accumulation in Channel 1 is a non-linear
303 relationship. The observations at 0.5 N and 1.0 N implies that, in a range of concentration
304 of nutrient, the biofilm growth rate is independent of the nutrient concentration in the
305 beginning of biofilm growth (29); as biofilm growing in size, biomass demand is rising
306 steadily, thereby the nutrient concentration determinates the growth rate in the later stage
307 of biofilm development.
308 Biofilm accumulation in Channel 2 increased with shear rate and nutrient concentration
309 in Channel 1 monotonically. Due to in absence of shear stress, biofilm growth in Channel
310 2 depends on the nutrient diffusive flux from Channel 1, which increases with the flow
311 velocity and nutrient concentration. Therefore, for a confined no flowing system, biofilm

accumulation rate is highly related to the nutrients availability, while the flow shear rate facilitates mass transfer, leading to an increase in biofilm accumulation. These observations are in correspondence with previous works (20, 21, 37).

The results indicates that for porous systems, like oil reservoirs, biofilm could develop not only in the main water flow paths, but also in dead ends and less flooded areas. Therefore, optimized nutrient flow velocity and nutrient concentration ensures sufficient nutrients supplying rate with moderate shear stress in the microchannel, resulting in biofilm accumulation in both flowing and non-flow regions.

Biofilm adhesive strength with the glass surface. Since only the nutrients solution was injected through Channel 1 after bacterial inoculation, the suspended cells in the effluent can be interpreted as the detachment of biofilms which dispersed their planktonic cells in the bulk growth medium. During exposure to stress, including shear stress and nutrient starvation, cells dispersed from biofilms go into the planktonic growth phase (39, 40). In this study, we observed that the biofilm-dispersal cells increased with flow velocity due to the shear stress induced detachment; nutrient starvation was also a trigger for biofilm dispersal. In addition to poor nutrient loading, biofilms culturing at the high nutrient concentration (2.0 N in this study) could also result in biofilm dispersal in the deep of biofilm matrix, which is mainly because that cells trapped deeper in the biofilm matrix may have difficulties obtaining essential sources of energy or nutrients. In a flowing system, biofilm dispersal is beneficial to spawn novel biofilm development cycles at new locations. Therefore, biofilm dispersal can potentially be used to control bioplugging in the further places of porous media.

In contrast to the planktonic mode, biofilm in a self-generated matrix can behave as viscous liquids to resist the flow shear stress and prevent from detachment from the attached solid surface. The results from biofilm adhesive strength test have demonstrated that biofilms growing at medium nutrient concentrations (0.5 N and 1.0 N) could resist the flow-induced shear stress. Compared to the large detachment at the initial stage, it suggests that the adhesive strength between biofilms and adhesive surface became stronger under shear (22, 41, 42). However, biofilm growth at high nutrient concentration (2.0 N) forms a loose structure with a high accumulation rate but a weak adhesive strength with substrates, which is easily detached by fluid shear.

In conclusion, this work demonstrates that flow velocity and nutrient concentrations can have significant impacts on biofilm development in both flowing and stagnant microchannels. Negligible biofilm formation at the relatively high flow velocity of 4.17 mm/s and low nutrient concentration of 0.1 N suggests that there is a 'no/low growth region', where high shear forces lead to biofilm detachment and nutrient concentration is below the minimum required for biofilm formation. This is supported by the earlier work (21). At the conditions investigated in this work, a strong plugging effect in the flowing microchannel was obtained at the relatively low flow velocity of 1.66 mm/s and the medium nutrient concentration of 1.0 N (10 mM substrate), which has a relative fast biofilms accumulation rate and a strong adhesion force to resist increase in the flow-induced shear. This research gives new insight to the relative influences of flow velocity and nutrient concentration on biofilms development at pore scale. This may aid evaluations of bioplugging in porous systems such as for oil and ground water reservoirs. As potential permeability reducers in oil reservoirs, biofilm accumulation in porous

357 media needs to be controlled by flow velocity and nutrient availability. Optimized
358 nutrient flow velocity and concentration ensures sufficient nutrients supplying rate with
359 moderate shear stress in the microchannel, resulting in biofilm accumulation in both
360 flowing and non-flow regions. However, too high stress may prevent biofilm formation
361 and removal of adhered biofilms in the porous media. High nutrient concentration is
362 beneficial for biofilm growth, but leads to a weak biofilm adhesive strength, which is
363 easily detached by flow shear from the pores.

364 **MATERIALS AND METHODS**

365 **Bacteria and fluids**. The bacteria used in the study was: *Thalassospira strain A216101*, a
366 facultative anaerobic, nitrate-reducing bacteria (NRB), capable of growing under both
367 aerobic and anaerobic conditions. It is able to grow on fatty acids and other organics
368 acids as sole carbon and energy source. Bacteria were enriched in a marine mineral
369 medium, which contained the following components (L^{-1}): 0.02 g Na_2SO_4, 1.00 g
370 KH_2PO_4, 0.10 g NH_4Cl, 20.00 g NaCl, 3.00 g $MgCl_2 \cdot 6H_2O$, 0.50 g KCl, 0.15 g
371 $CaCl_2 \cdot 2H_2O$, 0.70 g $NaNO_3$, and 0.50 ml 0.20% resazurin (43). The medium is hereafter
372 referred to as growth medium. After autoclaving in a dispenser, 1 L of growth medium
373 was added 5 ml vitamin solution and 20 ml 1 M $NaHCO_3$ to adjust the pH to 6.80-7.20.
374 Finally, pyruvate was added as the carbon source from a sterile stock solution to achieve
375 final nutrient concentrations of 20 mM (2.0 N), 10 mM (1.0 N), 5 mM (0.5 N), and 1 mM
376 (0.1 N), respectively. The final nutrient medium was stored at 4°C.

377 **Experimental setup.** The experimental apparatus is illustrated in **Fig. 1**. A T-junction
378 microfluidic device (Micronit, Netherland) consists of a single straight channel and a side
379 channel with the sizes of 100 μm width and 20 μm depth and the nuzzle size at the cross-

section as narrow as 10 μm (**Fig. S1**). Two syringe pumps (NE-1000 Series of Syringe Pumps, accuracy ±1%) were used to load the bacterial inoculation solution and nutrients solution separately into the microchannels. The light source is a cold halogen lamp with 24v, 150w placed under the microchip for better illumination. The micromodel was then placed under a microscope with a digital camera (VisiCam 5.0, VWR) to acquire image sequences. Measurements and experiments were conducted at room temperature and pressure.

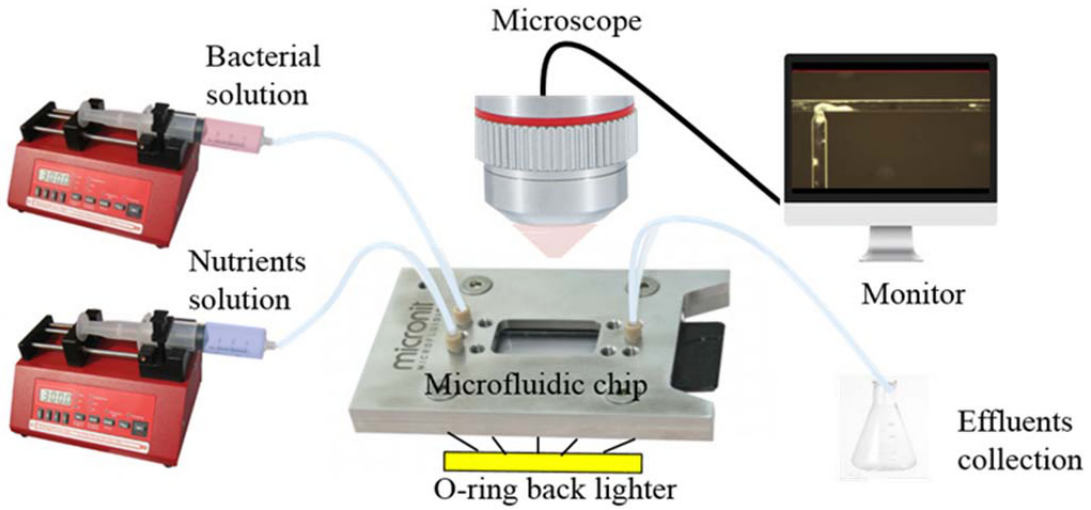

FIG 1. Schematic illustration of the experimental setup.

Inoculation process. Before inoculation, the microchannel was cleaned using ethyl alcohol, deionized water, H_2O_2 solution (10 wt%) and deionized water to guarantee the same surface condition for each experiment. The bacterial inocula were pre-cultured in the growth medium containing 10 mM (1.0 N) nutrients at 30 °C for 24 h. Inoculation was achieved by injecting the pre-culture bacterial solution from the bacterial inlet port (**Fig. S1 (a)**) into the side channel at the rate of 1.0 μl/min for 24 h, followed by a 24 h shut-in period. In case of biofilm clogging the straight channel for nutrients injection, we

separated the bacterial injection channel (Channel 2) and nutrients flowing channel (Channel 1) and closed the nutrient inlet during inoculation to force bacterial solution to only flow towards the outlet direction. Then only nutrients with various pyruvate concentrations (from 0.1 N to 2.0 N) were injected from the nutrients flow channel (Channel 1) at constant flowrates from 0.2 to 0.5 µl/min for approximately 6-7 days, while Channel 2 was closed, which led to a greater growing of bacteria on the substrates of the intersection of straight channel and side channel. Before the next experiment, microchannels were rinsed with ethyl alcohol, water, H_2O_2 solution and water separately, finally, filled with the marine medium without nutrients until the onset of the next experiment.

Image process. Image sequences on biofilm growth were acquired with a Leica microscope fitted with a digital camera for scoring with time. The main area of interest in this study is the intersection of straight channel and side channel, thereby two areas of interest (AOIs) with 0.5mm*0.1mm are extracted from the origin image for further image analysis (**Figure S1 (b)**). The image processing was performed using MATLAB®'s Image Processing Toolbox. Biofilm accumulation, here presented by biofilm coverage (A_{nt}) in areas of interest, was periodically measured in a flowing channel (Channel 1) and no-flowing channel (Channel 2). Further details on image process can be found in Support Information S1.

Effluent PCR analysis. Fluid samples were collected daily at the outlet through a quantitative real-time PCR (qPCR) on whole-cells to determine the total number of bacteria. A 20 µl qPCR reaction mix containing 10 µl SYBR® Green PCR kit, 0.06 µl primers (100uM), 8.88 µl nuclease free water and 1 µl template was made. The reaction

was run by the following cycling conditions: denaturation of DNA at 95°C for 15 minutes, 36 cycles with denaturation for 30 seconds at 94°C, annealing for 30 seconds at 55°C, extension for 1 minute at 72°C followed by a plate read. At the end, a melting curve from 55°C to 95°C was conducted. The reactions were carried out in a CFX connect™ real time PCR detection system (BioRad).

ACKNOWLEDGMENTS

We wish to thank Edin Alagic, Rikke H. Ulvøen and Tove L. Eide for technical assistance. This work was supported by the Research Council of Norway and industry partner GOE-IP through the projects IMMENS no. 255426.

REFERENCES

1. Karambeigi MS, Schaffie M, Fazaelipoor MH, Saadat M. 2009. Micromodel Studies of Bioplugging Efficiency in Heterogeneous Porous Media by Means of Mixed Culture of Microorganisms, Abstr 1st International Petroleum Conference and Exhibition Shiraz 2009, Shiraz, Iran.
2. Karambeigi MS, Schaffie M, Fazaelipoor MH. 2013. Improvement of Water Flooding Efficiency Using Mixed Culture of Microorganisms in Heterogeneous Micro-models. Pet. Sci. Technol. 31:923-931.
3. Peszynska M, Trykozko A, Iltis G, Schlueter S, Wildenschild D. 2016. Biofilm growth in porous media: Experiments, computational modeling at the porescale, and upscaling. Adv. Water Resour. 95:288-301.
4. Dumitrache A, Wolfaardt G, Allen G, Liss SN, Lynd LR. 2013. Form and function of Clostridium thermocellum biofilms. Appl. Environ. Microbiol. 79:231-9.

442 5. Vilcáez J, Li L, Wu D, Hubbard SS. 2013. Reactive Transport Modeling of
443 Induced Selective Plugging byLeuconostoc Mesenteroidesin Carbonate
444 Formations. Geomicrobiol. J. 30:813-828.
445 6. Joshi S, Goyal S, Mukherjee A, Reddy MS. 2017. Microbial healing of cracks in
446 concrete: a review. J. Ind. Microbiol. Biotechnol. 44:1511-1525.
447 7. Oka GK, Pinder GF. 2017. Multiscale Model for Assessing Effect of Bacterial
448 Growth on Intrinsic Permeability of Soil: Model Description. Transp. Porous
449 Media 119:267-284.
450 8. Alhede M, Qvortrup K, Liebrechts R, Hoiby N, Givskov M, Bjarnsholt T. 2012.
451 Combination of microscopic techniques reveals a comprehensive visual
452 impression of biofilm structure and composition. FEMS Immunol. Med.
453 Microbiol. 65:335-42.
454 9. Manuel CM, Nunes OC, Melo LF. 2007. Dynamics of drinking water biofilm in
455 flow/non-flow conditions. Water Res. 41:551-62.
456 10. Brovelli A, Malaguerra F, Barry DA. 2009. Bioclogging in porous media: Model
457 development and sensitivity to initial conditions. Environmental Modelling &
458 Software 24:611-626.
459 11. Karimi M, Mahmoodi M, Niazi A, Al-Wahaibi Y, Ayatollahi S. 2012.
460 Investigating wettability alteration during MEOR process, a micro/macro scale
461 analysis. Colloids Surf., B 95:129-36.
462 12. Khajepour H, Mahmoodi M, Biria D, Ayatollahi S. 2014. Investigation of
463 wettability alteration through relative permeability measurement during MEOR
464 process: A micromodel study. J. Pet. Sci. Eng. 120:10-17.

13. Hosseininoosheri P, Lashgari HR, Sepehrnoori K. 2016. A novel method to model and characterize in-situ bio-surfactant production in microbial enhanced oil recovery. Fuel 183:501-511.

14. Rabiei A, Sharifinik M, Niazi A, Hashemi A, Ayatollahi S. 2013. Core flooding tests to investigate the effects of IFT reduction and wettability alteration on oil recovery during MEOR process in an Iranian oil reservoir. Appl. Microbiol. Biotechnol. 97:5979-91.

15. Sarafzadeh P, Niazi A, Oboodi V, Ravanbakhsh M, Hezave AZ, Ayatollahi SS, Raeissi S. 2014. Investigating the efficiency of MEOR processes using Enterobacter cloacae and Bacillus stearothermophilus SUCPM#14 (biosurfactant-producing strains) in carbonated reservoirs. J. Pet. Sci. Eng. 113:46-53.

16. Brown LR. 2010. Microbial enhanced oil recovery (MEOR). Curr. Opin. Microbiol. 13:316-20.

17. Suthar H, Krushi Hingurao, Anjana Desai, Nerurkar aA. 2009. Selective Plugging Strategy Based Microbial Enhanced Oil Recovery Using Bacillus licheniformis TT33. J. Microbiol. Biotechnol. 19:8.

18. Klueglein N, Kögler F, Adaktylou IJ, Wuestner ML, Mahler E, Scholz J, Herold A, Alkan H. 2016. Understanding Selective Plugging and Biofilm Formation of a Halophilic Bacterial Community for MEOR Application. Soc. Pet. Eng. J. SPE-179620-MS.

19. Tsai YP. 2005. Impact of flow velocity on the dynamic behaviour of biofilm bacteria. Biofouling 21:267-77.

20. Rozen R, Bachrach G, Zachs B, Steinberg D. 2001. Growth rate and biofilm thickness of Streptococcus sobrinus and Streptococcus mutans on hydroxapatite. APMIS 109:6.

21. P. Stoodley ID, J.D.Boyle and H.M. Lappin-Scott. 1999. Influence of hydrodynamics and nutrients on biofilm structure. J. Appl. Microbiol. 85:7.

22. Flemming H-C, Wingender J, Szewzyk U. 2011. Biofilm highlights, vol 5, Heidelberg, USA.

23. Abdel Aal GZ, Atekwana EA, Atekwana EA. 2010. Effect of bioclogging in porous media on complex conductivity signatures. J. Geophys. Res. 115.

24. Cuzman OA, Rescic S, Richter K, Wittig L, Tiano P. 2015. Sporosarcina pasteurii use in extreme alkaline conditions for recycling solid industrial wastes. J. Biotechnol. 214:49-56.

25. Guimera X, Moya A, Dorado AD, Villa R, Gabriel D, Gabriel G, Gamisans X. 2015. Biofilm dynamics characterization using a novel DO-MEA sensor: mass transport and biokinetics. Appl. Microbiol. Biotechnol. 99:55-66.

26. Lee JH, Kaplan JB, Lee WY. 2008. Microfluidic devices for studying growth and detachment of Staphylococcus epidermidis biofilms. Biomed. Microdevices 10:489-98.

27. Weiss N, Obied KE, Kalkman J, Lammertink RG, van Leeuwen TG. 2016. Measurement of biofilm growth and local hydrodynamics using optical coherence tomography. Biomed. Opt. Express 7:3508-3518.

508 28. Hunt SM, Werner EM, Huang B, Hamilton MA, Stewart PS. 2004. Hypothesis for
509 the role of nutrient starvation in biofilm detachment. Appl. Environ. Microbiol.
510 70:7418-25.
511 29. Rochex A, Lebeault JM. 2007. Effects of nutrients on biofilm formation and
512 detachment of a Pseudomonas putida strain isolated from a paper machine. Water
513 Res. 41:2885-92.
514 30. Cherifi T, Jacques M, Quessy S, Fravalo P. 2017. Impact of Nutrient Restriction
515 on the Structure of Listeria monocytogenes Biofilm Grown in a Microfluidic
516 System. Front Microbiol. 8:864.
517 31. Rukavina Z, Vanic Z. 2016. Current Trends in Development of Liposomes for
518 Targeting Bacterial Biofilms. Pharmaceutics 8.
519 32. Skolimowski M, Nielsen MW, Emneus J, Molin S, Taboryski R, Sternberg C,
520 Dufva M, Geschke O. 2010. Microfluidic dissolved oxygen gradient generator
521 biochip as a useful tool in bacterial biofilm studies. Lab Chip 10:2162-9.
522 33. Tahirbegi IB, Ehgartner J, Sulzer P, Zieger S, Kasjanow A, Paradiso M, Strobl M,
523 Bouwes D, Mayr T. 2017. Fast pesticide detection inside microfluidic device with
524 integrated optical pH, oxygen sensors and algal fluorescence. Biosens.
525 Bioelectron. 88:188-195.
526 34. Raudales RE, Parke JL, Guy CL, Fisher PR. 2014. Control of waterborne
527 microbes in irrigation: A review. Agric. Water Manag. 143:9-28.
528 35. Lam RH, Cui X, Guo W, Thorsen T. 2016. High-throughput dental biofilm
529 growth analysis for multiparametric microenvironmental biochemical conditions
530 using microfluidics. Lab Chip 16:1652-62.

531 36. Sekar R, Nair KVK, Rao VNR, Venugopalan VP. 2002. Nutrient dynamics and
532 successional changes in a lenticfreshwater biofilm. Freshwater Biol. 47:14.
533 37. Bester E, Wolfaardt G, Joubert L, Garny K, Saftic S. 2005. Planktonic-cell yield
534 of a pseudomonad biofilm. Appl. Environ. Microbiol. 71:7792-8.
535 38. Kirby BJ. 2010. Passive Scalar Transport: Dispersion, Patterning, and Mixing,
536 Micro- and Nanoscale Fluid Mechanics: Transport in Microfluidic Devices
537 doi:https://doi.org/10.1017/CBO9780511760723.006. Cambridge University
538 Press, New York.
539 39. Gjermansen M, Nilsson M, Yang L, Tolker-Nielsen T. 2010. Characterization of
540 starvation-induced dispersion in Pseudomonas putida biofilms: genetic elements
541 and molecular mechanisms. Mol. Microbiol. 75:815-26.
542 40. Chua SL, Liu Y, Yam JKH, Chen Y, Vejborg RM, Tan BGC, Kjelleberg S,
543 Tolker-Nielsen T, Givskov M, Yang L. 2014. Dispersed cells represent a distinct
544 stage in the transition from bacterial biofilm to planktonic lifestyles. Nat.
545 Commun. 5.
546 41. Ohashi A, Harada H. 1994. Adhesion strength of biofilm developed in an
547 attached-growth reactor. Water Sci. Technol. 29:8.
548 42. Billings N, Birjiniuk A, Samad TS, Doyle PS, Ribbeck K. 2015. Material
549 properties of biofilms-a review of methods for understanding permeability and
550 mechanics. Rep. Prog. Phys. 78:036601.
551 43. Myhr S, Lillebo BL, Sunde E, Beeder J, Torsvik T. 2002. Inhibition of microbial
552 H2S production in an oil reservoir model column by nitrate injection. Appl.
553 Microbiol. Biotechnol. 58:400-8.

554